ORIGINAL RESEARCH

Prediction Model for in-Stent Restenosis Post-PCI Based on Boruta Algorithm and Deep Learning: The Role of Blood Cholesterol and Lymphocyte Ratio

Ling Hou[1,2,*], Ke Su[1,*], Ting He[1], Jinbo Zhao[1], Yuanhong Li[1]

[1]Cardiovascular Disease Center, Central Hospital of Tujia and Miao Autonomous Prefecture, Hubei University of Medicine, Enshi, Hubei Province, People's Republic of China; [2]Department of Central Hospital of Tujia and Miao Autonomous Prefecture, Hubei University of Medicine, Shiyan, Hubei Province, People's Republic of China

*These authors contributed equally to this work

Correspondence: Yuanhong Li, Email lyh0101@vip.163.com

Background: Percutaneous coronary intervention (PCI) is the primary treatment for acute myocardial infarction (AMI). However, in-stent restenosis (ISR) remains a significant limitation to the efficacy of PCI. The cholesterol-to-lymphocyte ratio (CLR), a novel biomarker associated with inflammation and dyslipidemia, may have predictive value for ISR. Deep learning-based models, such as the multilayer perceptron (MLP), can aid in establishing predictive models for ISR using CLR.

Methods: A retrospective analysis was conducted on clinical and laboratory data from 1967 patients. The Boruta algorithm was employed to identify key features associated with ISR. An MLP model was developed and divided into training and validation sets. Model performance was evaluated using ROC curves and calibration plots.

Results: Patients in the ISR group exhibited significantly higher levels of CLR and low-density lipoprotein (LDL) compared to the non-ISR group. The Boruta algorithm identified 21 important features for subsequent modeling. The MLP model achieved an AUC of 0.95 on the validation set and 0.63 on the test set, indicating good predictive performance. Calibration plots demonstrated good agreement between predicted and observed outcomes. Feature importance analysis revealed that the number of initial stent implants, hemoglobin levels, Gensini score, CLR, and white blood cell count were significant predictors of ISR. Partial dependence plots (PDP) confirmed CLR as a key predictor for ISR.

Conclusion: The CLR, as a biomarker that integrates lipid metabolism and inflammation, shows significant potential in predicting coronary ISR. The MLP model, based on deep learning, demonstrated robust predictive capabilities, offering new insights and strategies for clinical decision-making.

Keywords: cholesterol-to-lymphocyte ratio, deep learning, multilayer perceptron, Boruta algorithm, in-stent restenosis

Background

Acute myocardial infarction (AMI) is a severe cardiovascular condition associated with high morbidity and mortality due to complications such as congestive heart failure and malignant arrhythmias.[1] Percutaneous coronary intervention (PCI) is a primary treatment for AMI,[2] yet its efficacy is often hampered by the occurrence of in-stent restenosis (ISR).[3] ISR, characterized by the re-narrowing of the treated vessel, can lead to stent failure, necessitating repeat interventions and adversely affecting patient outcomes.[4] Therefore, identifying strategies to reduce ISR incidence is crucial for improving the prognosis of AMI patients.

Previous studies have established that inflammation and dyslipidemia significantly contribute to ISR development.[5–11] Inflammatory responses can cause endothelial injury and proliferation, while abnormal lipid metabolism may accelerate

atherosclerosis, promoting ISR.[12,13] Traditional ISR prediction methods often rely on single biomarkers, which may lack accuracy and sensitivity. Consequently, there is a need to explore novel indicators and methods for ISR prediction. Blood cholesterol levels reflect lipid metabolism, and lymphocyte ratios indicate immune status. The cholesterol-to-lymphocyte ratio (CLR) is an emerging biomarker that encapsulates both lipid metabolism and inflammation,[14] potentially offering unique advantages in predicting ISR.

Other relevant factors such as age, gender, hypertension, diabetes mellitus, and smoking status may play significant roles in ISR risk. Previous research has highlighted that advanced age and male gender are associated with increased ISR rates.[15] Furthermore, hypertension and diabetes are well-known contributors to endothelial dysfunction, atherosclerosis, and subsequent ISR.[16] Smoking is another critical risk factor, as it exacerbates inflammation and accelerates the process of vascular injury.[17] By considering these clinical and demographic factors alongside CLR, this study can provide a more comprehensive model for ISR prediction.

Multilayer perceptron (MLP)-based deep learning models are powerful predictive tools capable of handling complex data relationships and non-linear modeling.[18] This study aims to investigate the impact of CLR on ISR in coronary stenting, providing new insights and strategies for clinical decision-making.

Methods

Study Population

This retrospective analysis encompassed 1967 patients from the Cardiology Department at Enshi Tujia and Miao Autonomous Prefecture Central Hospital, who underwent PCI followed by a subsequent coronary angiography between January 2022 and May 2024. Inclusion criteria were: (1) patients who had received coronary stent intervention with a postoperative period exceeding 90 days; (2) patients who underwent coronary angiography; (3) patients who regularly took antiplatelet and lipid-lowering medications. Exclusion criteria included: (1) patients who refused medication due to disease reasons (eg, bleeding, liver function abnormalities) or poor compliance; (2) patients with procedural factors during the initial PCI that could lead to restenosis within 90 days post-procedure; (3) patients excluded due to other diseases that might affect the study outcomes (tumors, embolism, rheumatic immune diseases); (4) patients with incomplete follow-up data (as shown in Figure 1). ISR was defined as a luminal diameter stenosis ≥50% within or at the stent edges (≤5 mm from the stent edge) using the distal vessel diameter as a reference.[19] This study, a retrospective observational study, was approved by the Ethics Committee of Enshi Tujia-Miao Autonomous Prefecture Central Hospital and adhered to the principles outlined in the Declaration of Helsinki. Due to the retrospective nature of the study, written informed consent was not required. Patient data confidentiality was strictly maintained, and all data were anonymized prior to analysis to protect patient privacy. No identifying information, such as names, addresses, or personal identifiers, was included in the dataset.
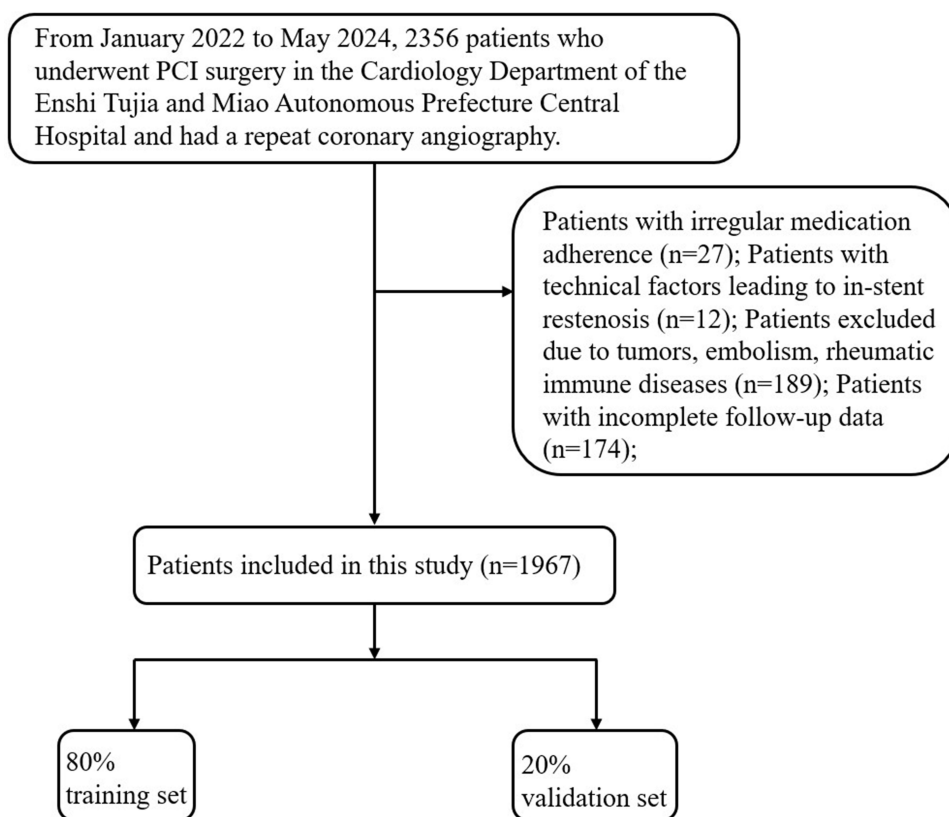
Data Collection

Clinical data were collected for all patients, including age, gender, smoking history, comorbidities (diabetes, hypertension, stroke), number of lesions, number of stents, stent length, stent diameter, and postoperative medication use (anticoagulants, diuretics). Fasting venous blood samples were collected in the morning for complete blood count, liver and kidney function tests, and lipid profile. CLR was calculated by dividing the total cholesterol by the absolute lymphocyte count.[14]

Feature Selection

We utilized the Boruta algorithm to identify the most critical baseline features associated with ISR. The Boruta algorithm, an extension of the random forest algorithm, determines important features by comparing original features with randomly shuffled "shadow" features to predict the target variable.[20]

Deep Learning Model Development

The multilayer perceptron (MLP), a foundational model in deep learning, consists of multiple neuron layers interconnected by weights. By stacking multiple neural network layers and incorporating nonlinear activation functions, MLPs

From January 2022 to May 2024, 2356 patients who underwent PCI surgery in the Cardiology Department of the Enshi Tujia and Miao Autonomous Prefecture Central Hospital and had a repeat coronary angiography.

Patients with irregular medication adherence (n=27); Patients with technical factors leading to in-stent restenosis (n=12); Patients excluded due to tumors, embolism, rheumatic immune diseases (n=189); Patients with incomplete follow-up data (n=174);

Patients included in this study (n=1967)

80% training set

20% validation set

Figure 1 Flowchart of the detailed selection process.

can learn complex feature representations, thereby enhancing model accuracy and generalization capabilities. We employed an 8:2 training-validation split to leverage a larger dataset for learning more features and patterns, thereby improving model performance. We plotted ROC curves and calibration curves to compare model performance on training and test sets, analyzing prediction accuracy and reliability. Feature importance plots visually represented the contribution of different features to ISR. Finally, we used Partial Dependence Plots (PDP) to examine the interaction between ISR and various features, revealing the complex relationships and their impact on model predictions.

Statistical Analysis

Statistical analyses were conducted using R version 4.3.3 and Python version 3.9. Continuous variables with normal distribution were expressed as mean ± standard deviation, while categorical variables were expressed as percentages. A two-tailed p-value of less than 0.05 was considered statistically significant.

Results
Baseline Characteristics

As shown in Table 1, there was no significant difference in age between the groups, although the mean age of patients in the ISR group was 64 years, slightly higher than the 63 years in the non-ISR group. A significant gender difference was observed, with a higher proportion of males in the ISR group compared to the non-ISR group (83.8% vs 72.1%, P < 0.001). There were no significant differences between the groups regarding baseline comorbidities such as diabetes, hypertension, and stroke. Clinically, the ISR group had a significantly higher proportion of smokers compared to the non-ISR group (P = 0.001). Regarding coronary artery lesion locations, the ISR group had significantly higher rates of lesions in the left anterior descending, left circumflex, and right coronary arteries. Additionally, the ISR group exhibited a higher number of diseased vessels and Gensini scores than the non-ISR group. In laboratory indices, most parameters (including

Table 1 Descriptive Characteristics of Overall Participants

| Variable	no ISR(n=1633)	ISR(n=334)	P-value
age (median [IQR])	63.00 [55.00, 70.00]	64.00 [56.00, 70.00]	0.149
Sex =1 (%)	1177 (72.1)	280 (83.8)	<0.001*
hypertension =1 (%)	915 (56.0)	176 (52.7)	0.264
Diabetes=1 (%)	406 (24.9)	95 (28.4)	0.171
Stroke=1 (%)	167 (10.2)	35 (10.5)	0.89
smoking=1 (%)	858 (52.5)	209 (62.6)	0.001*
anticoagulant=1 (%)	510 (31.2)	88 (26.3)	0.077
Diuretic (%)	269 (16.5)	55 (16.5)	0.998
Left main stem=1 (%)	122 (7.5)	35 (10.5)	0.065
Left anterior descending branch=1 (%)	1323 (81.0)	296 (88.6)	0.001*
Left Circumflex branch=1 (%)	1015 (62.2)	239 (71.6)	0.001*
Right Circumflex branch=1 (%)	1069 (65.5)	253 (75.7)	<0.001*
Number of diseased vessels (median [IQR])	40.00 [20.00, 64.00]	52.00 [34.00, 89.00]	<0.001*
Gensini scores (median [IQR])	1.00 [1.00, 2.00]	2.00 [1.00, 3.00]	0.035*
length (median [IQR])	3.00 [2.75, 3.50]	3.00 [2.75, 3.50]	0.283
width (median [IQR])	29.00 [21.00, 35.00]	25.00 [21.00, 33.00]	0.608
WBC (median [IQR])	6.17 [5.14, 7.62]	6.36 [5.36, 7.71]	0.126
Neutrophils (median [IQR])	3.97 [3.11, 5.16]	4.12 [3.21, 5.37]	0.093
Monocyte (median [IQR])	0.38 [0.30, 0.48]	0.39 [0.32, 0.51]	0.069
Hemoglobin (median [IQR])	138.00 [127.00, 150.00]	139.00 [128.25, 149.00]	0.688
Platelets (median [IQR])	182.00 [151.00, 219.00]	178.00 [150.00, 215.00]	0.643
Platelet Distribution Width (median [IQR])	16.30 [16.10, 16.50]	16.30 [16.00, 16.50]	0.421
Aspartate Aminotransferase (median [IQR])	24.00 [20.00, 33.00]	24.00 [21.00, 33.00]	0.652
Direct Bilirubin (median [IQR])	3.30 [2.30, 4.40]	3.40 [2.20, 4.60]	0.439
Creatinine (median [IQR])	73.30 [61.70, 87.90]	72.05 [61.90, 86.95]	0.663
Random Blood Glucose (median [IQR])	5.23 [4.59, 6.46]	5.20 [4.59, 6.48]	0.789
Uric acid (median [IQR])	348.37 [290.10, 414.29]	348.24 [293.50, 410.87]	0.73
CLR (median [IQR])	2.61 [1.93, 3.55]	2.82 [1.99, 3.79]	0.046*
Triglyceride (median [IQR])	1.29 [0.95, 1.85]	1.36 [0.99, 1.81]	0.587
High-Density Lipoprotein (median [IQR])	1.03 [0.88, 1.19]	1.02 [0.87, 1.22]	0.765
Low-Density Lipoprotein (median [IQR])	2.32 [1.85, 2.90]	2.41 [1.96, 3.03]	0.04*
Thyroid Stimulating Hormone (median [IQR])	2.23 [1.47, 3.52]	2.37 [1.47, 3.73]	0.318

Note: *P<0.05.

leukocytes, neutrophils, monocytes, hemoglobin, platelets, platelet distribution width, aspartate aminotransferase, direct bilirubin, creatinine, random blood glucose, uric acid, triglycerides, high-density lipoprotein, and thyroid-stimulating hormone) showed no significant differences between the groups. However, the ISR group had significantly higher CLR and LDL levels compared to the non-ISR group.

Feature Selection Using Boruta Algorithm

Figure 2 illustrates the feature selection results using the Boruta algorithm. In this algorithm, the green area represents important features that significantly contribute to the model's predictive performance. The red area indicates unimportant features with no significant contribution, while the yellow area represents tentative features that lie between important and unimportant. For accurate subsequent modeling, we selected only the important features (21 in total) from the green area.

Model Performance

Figure 3 presents the ROC curve (Receiver Operating Characteristic curve) and calibration curve for the MLP model. The AUC (Area Under the Curve) for the validation set was 0.95, and for the test set, it was 0.63, indicating satisfactory
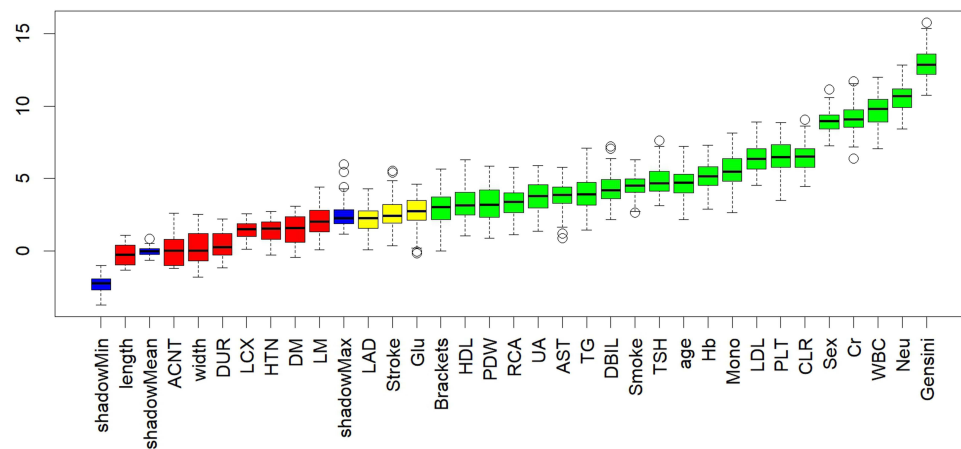
Figure 2 Feature selection based on Boruta algorithm (The green area indicates important features that significantly impact the model's predictions, while the red area shows unimportant features. The yellow area represents features of uncertain importance. The blue area represents the shadow features, which serve as a reference for determining the significance of the actual features).
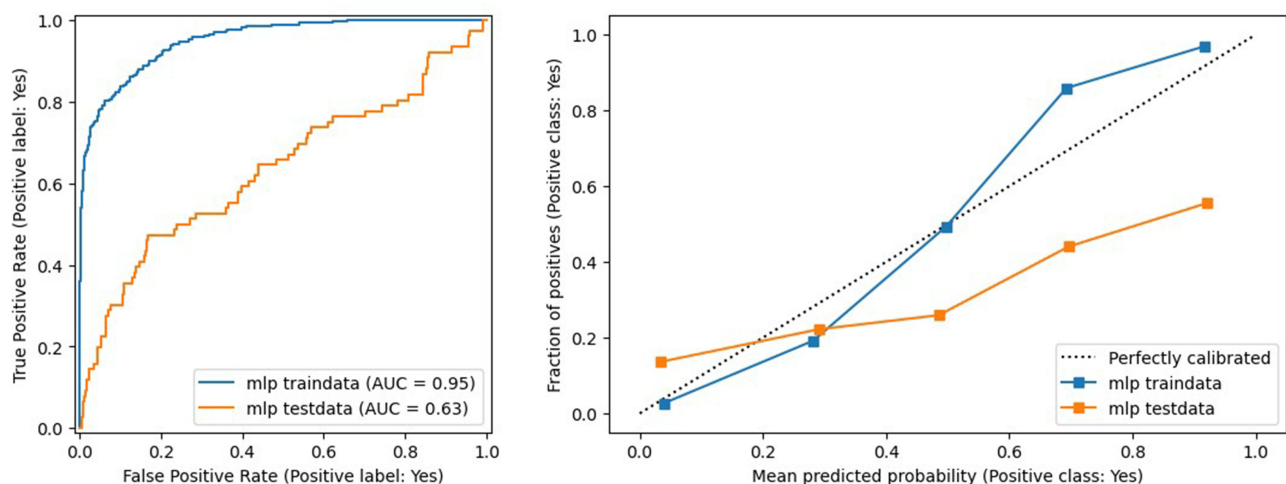

Figure 3 ROC curves and calibration curves of the training set and validation set.

model performance with good accuracy and sensitivity. Moreover, the calibration curve demonstrated good alignment between predictions and observations in both the training and test sets. Figure 4 displays the contribution of each variable to ISR occurrence, with the top five variables being the number of stents initially implanted, hemoglobin, Gensini score, CLR, and leukocytes. To further explore the relationship between CLR and ISR in the MLP model, we plotted PDP contour maps of CLR with the top four contributing variables: the number of stents initially implanted, hemoglobin, Gensini score, and leukocytes. As depicted in Figure 5, the contour maps clearly indicate that CLR is a critical variable in predicting ISR. Higher CLR values consistently corresponded to higher ISR probabilities across all variable combinations, highlighting CLR's significant role in prediction. Regardless of the values of other variables (Brackets, Gensini, Hb, WBC), an increase in CLR was always associated with an increased probability of ISR.

Discussion

Our research identified that the CLR plays a significant role in the occurrence of ISR. Using the Boruta algorithm for feature selection, we determined 21 important features for subsequent modeling. The MLP model demonstrated good predictive performance on both the validation and test sets. The model's calibration curve also showed a good agreement between predicted and actual outcomes. Further analysis revealed that the number of initial stent implants, hemoglobin
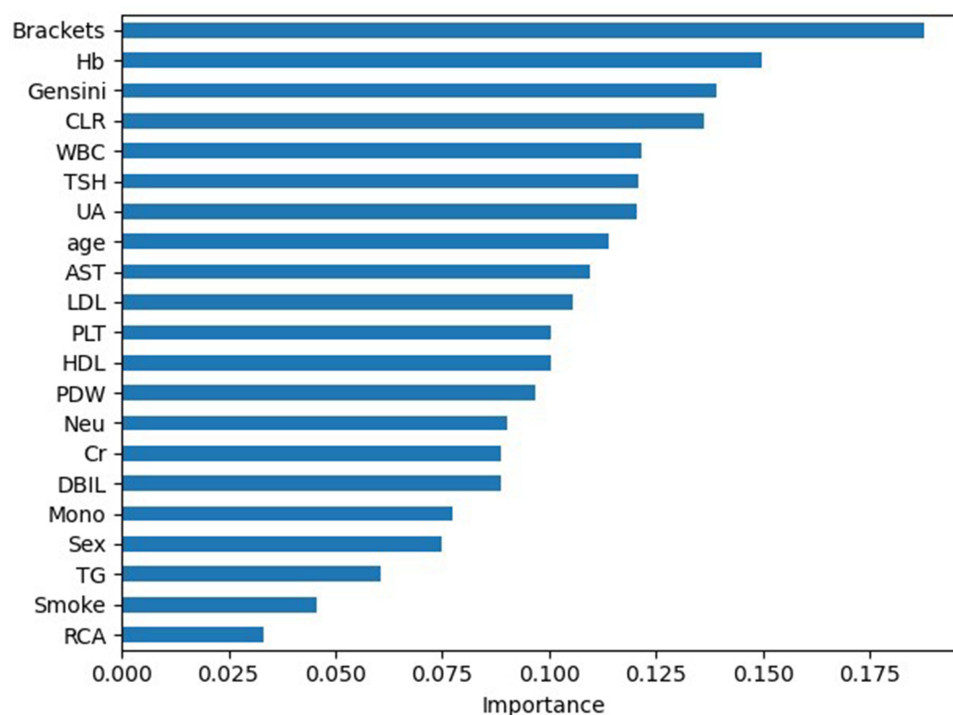
**Figure 4** Feature importance of variables in multilayer perceptron model.

levels, Gensini score, CLR, and white blood cell count were the five most significant variables contributing to ISR. Notably, contour plots illustrated CLR as a critical predictor of ISR, consistently showing an increased probability of ISR with higher CLR values, regardless of other variables.

Stent implantation disrupts the endothelial layer, leading to cholesterol and lipoprotein deposition, plaque formation, and an increased risk of thrombosis.[21] Lipid content within plaques induces inflammatory cell aggregation, releasing inflammatory factors that activate endothelial cells, exacerbating the inflammatory response.[22] Cholesterol deposits within plaques cause apoptosis and necrosis, releasing intracellular substances that further stimulate inflammation.[23] Plaque formation damages and ruptures the vascular wall, exposing tissue factors that promote platelet aggregation and thrombosis,[24] creating a vicious cycle leading to ISR.

The cholesterol-to-lymphocyte ratio provides a unique insight into the interplay between lipid metabolism and inflammation, both of which are critical drivers of ISR. Elevated CLR reflects higher cholesterol levels, contributing to lipid deposition and atherogenesis. This triggers an inflammatory cascade that exacerbates endothelial dysfunction and promotes neointimal hyperplasia, the primary pathological mechanism of ISR. Additionally, lymphocytes play a key role in modulating the immune response within the vascular system. Activated lymphocytes can increase local inflammation, leading to smooth muscle proliferation and plaque instability. This suggests that CLR, by capturing both lipid abnormalities and immune status, acts as a comprehensive marker of ISR risk.

Lymphocytes, as key cells in the inflammatory response, play a critical role in arterial wall inflammation.[25] Their activation and proliferation can exacerbate local inflammation, promote smooth muscle cell proliferation and migration, leading to neointimal hyperplasia,[26] a primary pathological mechanism of ISR. Therefore, high CLR levels may reflect enhanced inflammatory response, indicating a high risk of ISR. Elevated total cholesterol levels are a significant risk factor for atherosclerosis, as its deposition in the arterial wall leads to plaque formation and progression.[27] Although PCI can mechanically resolve coronary artery stenosis, high cholesterol levels may promote plaque regeneration and neointimal hyperplasia at the stent site,[28] increasing ISR incidence. CLR includes total cholesterol levels, thus indirectly reflecting the impact of lipid metabolism on ISR. Compared to single inflammatory markers (NLR, SII, SIRI, AISI) or lipid indicators (RC, TC/HDL-C, LDL-C/HDL-C, TG/HDL-C), CLR combines inflammation and lipid metabolism
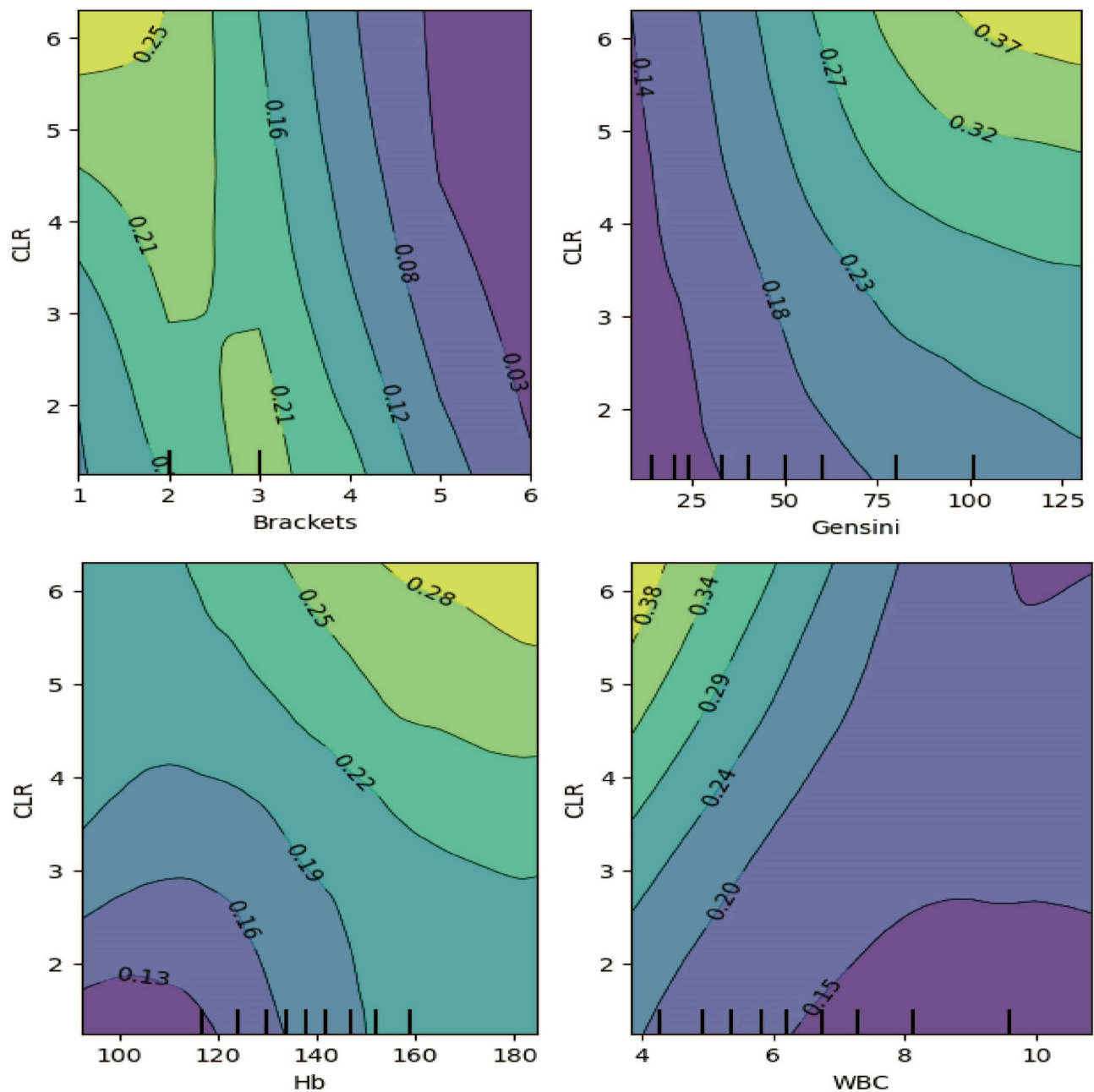
Figure 5 The synergistic effect of the main variables on in-stent restenosis.

aspects, providing a more comprehensive risk assessment. High CLR values may indicate more severe systemic inflammation and lipid abnormalities, jointly increasing ISR risk.

The activation of pro-inflammatory cytokines can mediate endothelial damage, further impairing vascular healing following PCI. High levels of cholesterol exacerbate oxidative stress and lipid peroxidation within the arterial wall, fostering a pro-thrombotic environment. This, in turn, promotes smooth muscle cell migration and proliferation, driving restenosis. Therefore, the dual contribution of high cholesterol and immune activation, as reflected by CLR, underscores its relevance in predicting ISR. CLR, by encompassing these key biological pathways, is not only a marker but potentially a contributor to ISR pathophysiology.

Previous studies have primarily used CLR to evaluate adverse prognosis in cancer patients post-surgery.[14,29] Our study is the first to describe the association between CLR and cardiovascular events. In clinical practice, CLR can serve

as a simple and accessible indicator, helping healthcare providers more accurately predict ISR risk. Regular monitoring of CLR levels in patients can facilitate early identification of high-risk individuals and the implementation of more aggressive preventive measures, such as intensified anti-inflammatory and lipid-lowering treatments, optimizing post-PCI management strategies to improve long-term outcomes.

Compared to our previous study,[30] this research utilizes data collected from a different time period and excludes data from patients with repeat hospital admissions. We employed the Boruta algorithm for feature selection and integrated it with a deep learning model to enhance the precision of predicting post-PCI in-stent restenosis. Additionally, this study places a specific emphasis on the roles of blood cholesterol and lymphocyte ratios in the prediction model, aspects that were not extensively explored in our prior work. These innovations highlight the robustness and applicability of our model in clinical settings, providing a more precise and comprehensive tool for predicting ISR risk.

However, the observed discrepancy in AUC scores between the validation (0.95) and test sets (0.63) may stem from overfitting, where the model performs exceptionally well on the training data but struggles to generalize to new data. Differences in patient characteristics between the training and test sets, along with the smaller size of the test set, could also contribute to this variance. Addressing these issues in future work will be crucial for improving model robustness and predictive accuracy.

Conclusion

As a novel biomarker reflecting both inflammation and lipid metabolism, CLR shows significant potential in predicting in-stent restenosis. Further large-scale clinical studies are warranted to validate the predictive value of CLR and explore its application prospects in cardiovascular disease management.

Disclosure

The authors report no conflicts of interest in this work.

References

1. Jernberg T, Hasvold P, Henriksson M, Hjelm H, Thuresson M, Janzon M. Cardiovascular risk in post-myocardial infarction patients: nationwide real world data demonstrate the importance of a long-term perspective. *Eur Heart J*. 2015;36(19):1163–1170. doi:10.1093/eurheartj/ehu505
2. Hoole SP, Bambrough P. Recent advances in percutaneous coronary intervention. *Heart*. 2020;106(18):1380–1386. doi:10.1136/heartjnl-2019-315707
3. Marfella R, Sardu C, D'Onofrio N, et al. SGLT-2 inhibitors and in-stent restenosis-related events after acute myocardial infarction: an observational study in patients with type 2 diabetes. *BMC Med*. 2023;21(1):71. doi:10.1186/s12916-023-02781-2
4. Giustino G, Colombo A, Camaj A, et al. Coronary in-stent restenosis: JACC state-of-the-art review. *J Am Coll Cardiol*. 2022;80(4):348–372. doi:10.1016/j.jacc.2022.05.017
5. Hu W, Jiang J. Hypersensitivity and in-stent restenosis in coronary stent materials. *Front Bioeng Biotechnol*. 2022;10:1003322. doi:10.3389/fbioe.2022.1003322
6. McDonald RA, Halliday CA, Miller AM, et al. Reducing in-stent restenosis: therapeutic manipulation of miRNA in vascular remodeling and inflammation. *J Am Coll Cardiol*. 2015;65(21):2314–2327. doi:10.1016/j.jacc.2015.03.549
7. Chiu JJ, Chien S. Effects of disturbed flow on vascular endothelium: pathophysiological basis and clinical perspectives. *Physiol Rev*. 2011;91(1):327–387. doi:10.1152/physrev.00047.2009
8. Drachman DE, Simon DI. Inflammation as a mechanism and therapeutic target for in-stent restenosis. *Curr Atheroscler Rep*. 2005;7(1):44–49. doi:10.1007/s11883-005-0074-5
9. Fishbein I, Inamdar VV, Alferiev IS, et al. Hypercholesterolemia exacerbates in-stent restenosis in rabbits: studies of the mitigating effect of stent surface modification with a CD47-derived peptide. *Atherosclerosis*. 2024;390:117432. doi:10.1016/j.atherosclerosis.2023.117432
10. Cheng Y, Shibuya M, McGregor J, et al. Biological effect on restenosis and vascular healing of encapsulated paclitaxel nanocrystals delivered via coated balloon technology in the familial hypercholesterolaemic swine model of in-stent restenosis. *Euro Interv*. 2016;12(9):1164–1173. doi:10.4244/eijv12i9a188
11. Ohtani K, Egashira K, Nakano K, et al. Stent-based local delivery of nuclear factor-kappaB decoy attenuates in-stent restenosis in hypercholesterolemic rabbits. *Circulation*. 2006;114(25):2773–2779. doi:10.1161/circulationaha.105.582254
12. Lv J, Zeng J, Guo F, et al. Endothelial Cdc42 deficiency impairs endothelial regeneration and vascular repair after inflammatory vascular injury. *Respir Res*. 2018;19(1):27. doi:10.1186/s12931-018-0729-8
13. Gisterå A, Hansson GK. The immunology of atherosclerosis. *Nat Rev Nephrol*. 2017;13(6):368–380. doi:10.1038/nrneph.2017.51
14. Zhou S, He Q, Sheng N, Gong J, Ren J, Wang Z. Blood cholesterol-to-lymphocyte ratio as a novel prognostic marker to predict postoperative overall survival in patients with colorectal cancer. *World J Surg Oncol*. 2022;20(1):18. doi:10.1186/s12957-021-02471-4
15. Yi M, Wu L, Ke X. Prognostic value of high-sensitivity C-reactive protein in in-stent restenosis: a meta-analysis of clinical trials. *J Cardiovasc Dev Dis*. 2022;9(8). doi:10.3390/jcdd9080247

16. Petrie JR, Guzik TJ, Touyz RM. Diabetes, hypertension, and cardiovascular disease: clinical insights and vascular mechanisms. *Can J Cardiol.* 2018;34(5):575–584. doi:10.1016/j.cjca.2017.12.005

17. Messner B, Bernhard D. Smoking and cardiovascular disease: mechanisms of endothelial dysfunction and early atherogenesis. *Arterioscler Thromb Vasc Biol.* 2014;34(3):509–515. doi:10.1161/atvbaha.113.300156

18. Albaradei S, Thafar M, Alsaedi A, et al. Machine learning and deep learning methods that use omics data for metastasis prediction. *Comput Struct Biotechnol J.* 2021;19:5008–5018. doi:10.1016/j.csbj.2021.09.001

19. Kitta Y, Obata JE, Takano H, et al. Echolucent carotid plaques predict in-stent restenosis after bare metal stenting in native coronary arteries. *Atherosclerosis.* 2008;197(1):177–182. doi:10.1016/j.atherosclerosis.2007.03.021

20. Degenhardt F, Seifert S, Szymczak S. Evaluation of variable selection methods for random forests and omics data sets. *Brief Bioinform.* 2019;20 (2):492–503. doi:10.1093/bib/bbx124

21. Tesfamariam B. Targeting Rho kinase to restore endothelial barrier function following vascular scaffold implantation. *Drug Discov Today.* 2023;28 (7):103609. doi:10.1016/j.drudis.2023.103609

22. Libby P. Inflammation during the life cycle of the atherosclerotic plaque. *Cardiovasc Res.* 2021;117(13):2525–2536. doi:10.1093/cvr/cvab303

23. Fisher AL, Srole DN, Palaskas NJ, et al. Iron loading induces cholesterol synthesis and sensitizes endothelial cells to TNFα-mediated apoptosis. *J Biol Chem.* 2021;297(4):101156. doi:10.1016/j.jbc.2021.101156

24. Fitzgerald DJ. Vascular biology of thrombosis: the role of platelet-vessel wall adhesion. *Neurology.* 2001;57(5 Suppl 2):S1–4. doi:10.1212/wnl.57. suppl_2.s1

25. Saigusa R, Winkels H, Ley K. T cell subsets and functions in atherosclerosis. *Nat Rev Cardiol.* 2020;17(7):387–401. doi:10.1038/s41569-020-0352-5

26. Hui DY. Intimal hyperplasia in murine models. *Curr Drug Targets.* 2008;9(3):251–260. doi:10.2174/138945008783755601

27. Nordestgaard BG, Langsted A, Mora S, et al. Fasting is not routinely required for determination of a lipid profile: clinical and laboratory implications including flagging at desirable concentration cut-points-a joint consensus statement from the European atherosclerosis society and European federation of clinical chemistry and laboratory medicine. *Eur Heart J.* 2016;37(25):1944–1958. doi:10.1093/eurheartj/ehw152

28. Feng AN, Chen YL, Chen YT, Ding YZ, Lin SJ. Red wine inhibits monocyte chemotactic protein-1 expression and modestly reduces neointimal hyperplasia after balloon injury in cholesterol-Fed rabbits. *Circulation.* 1999;100(22):2254–2259. doi:10.1161/01.cir.100.22.2254

29. Deng Y, Chen Q, Chen J, et al. An elevated preoperative cholesterol-to-lymphocyte ratio predicts unfavourable outcomes in colorectal cancer liver metastasis patients receiving simultaneous resections: a retrospective study. *BMC Surg.* 2023;23(1):131. doi:10.1186/s12893-023-01988-7

30. Hou L, Zhao J, He T, Su K, Li Y. Machine learning-based prediction of in-stent restenosis risk using systemic inflammation aggregation index following coronary stent placement. *Risk Manag Healthc Policy.* 2024;17:1779–1786. doi:10.2147/rmhp.S468235